ACS Macro Letters

Letter

pubs.acs.org/macroletters

All-Polymer Solar Cell with High Near-Infrared Response Based on a Naphthodithiophene Diimide (NDTI) Copolymer

Erjun Zhou,[†,‡] Masahiro Nakano,[‡] Seiichiro Izawa,[‡] Junzi Cong,[‡] Itaru Osaka,[‡] Kazuo Takimiya,*[,‡] and Keisuke Tajima*[,‡,§]

[†]National Center for Nanoscience and Technology, No. 11 Beiyitiao, Zhongguancun, Beijing 100190, People's Republic of China

[‡]RIKEN Center for Emergent Matter Science (CEMS), 2-1 Hirosawa, Wako 351-0198, Japan

[§]Japan Science and Technology Agency (JST), Precursory Research for Embryonic Science and Technology (PRESTO), 4-1-8 Honcho, Kawaguchi, Saitama 332-0012, Japan

ABSTRACT: Polymer-blend solar cells (all-PSCs) based on a copolymer of naphthodithiophene diimide and bithiophene (PNDTI-BT-DT) as a near-infrared absorber as well as an electron acceptor were fabricated in combination with PTB7 as an electron donor. Notably, the external quantum efficiency spectra of the all-PSCs demonstrated photoresponse up to 900 nm with the efficiency of 25% at 800 nm, which is much higher than that for the previously reported all-PSCs. Power conversion efficiency as high as 2.59% was achieved under the irradiation of simulated solar light (AM1.5, 100 mW/cm^2). Both PNDTI-BT-DT and PTB7 formed a crystalline structure in the blend films similar to in the pristine films, leading to the efficient charge generation contributed from both polymers.

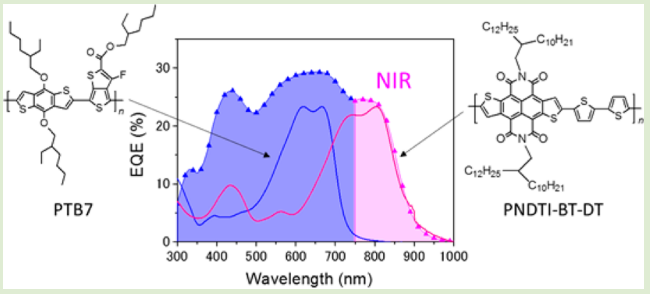

Polymer solar cells (PSCs) receive much attention in both academia and industry because of their versatile uses due to lightweight, mechanical flexibility and potential of low cost fabrication of large area devices through nonvacuum processes.[1] A bulk heterojunction (BHJ) type photoactive layer, in which a π-conjugated polymer as the donor and a fullerene derivative as the acceptor are phase separated in nanoscale, represents the most effective strategy to enlarge the interfacial area of the two materials for efficient charge separation. Fullerene derivatives are thus far the most common and effective electron acceptors due to their high electron affinity, relatively high mobility, and ability to induce ultrafast charge transfer and slow back transfer.[2]

Development of non-fullerene electron acceptors based on π-conjugated molecules and polymers opens up a possibility of designing new materials with high crystallinity, solubility, and tunable electronic properties, such as the light absorption and the frontier orbital energy levels, and thus further high PCEs.[3] In particular, the use of acceptors with long-wavelength absorption is expected to overcome the short-range absorption of the fullerene derivative, which may lead to the further improvement of PCEs. After the pioneering works on the polymer blend solar cells (or all-polymer solar cells; all-PSC) in 1995,[4] many π-conjugated polymers containing electron deficient moieties such as cyano groups,[5] 2,1,3-benzothiadiazole,[6] and diketopyrrolopyrrole[7] have emerged as potential electron acceptor materials for the application in all-PSCs. Among them, polymers with rylene diimides such as perylene diimide (PDI)[8] and naphthalene diimide (NDI)[9] (see Scheme 1) have been recognized as the most effective class of acceptor materials, with which PCEs in all-PSCs have reached over 5%. Although both the polymers can offer light absorption up to 1000 nm depending on the polymer structures, photocurrent responses of all-PSCs in near-infrared (NIR) region (>750 nm) is still quite low and typical EQE values are less than 5%,[8b,10] suggesting a small contribution of the acceptor absorption. Therefore, it still remains a challenge to develop the electron accepting polymers with long-wavelength absorption for better collection of the solar light.[11]

Scheme 1. n-Type Polymers Based on Three Rylene Diimide Building Blocks, PDI, NDI, and NDTI

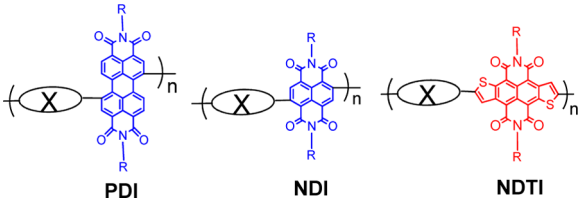

We recently developed a novel class of rylene dimide-based building block with an extended π-plane, naphtho[2,3-*b*:6,7-*b*′]dithiophenediimide (NDTI) (Scheme 1).[12] The polymer based on NDTI and bithiophene (PNDTI-BT-DT in Figure 1) has a coplanar backbone structure with extended absorption profile in NIR region up to 900 nm, and a lowest unoccupied

Received: July 14, 2014
Accepted: August 8, 2014
Published: August 18, 2014

   dx.doi.org/10.1021/mz5004272 | *ACS Macro Lett.* 2014, 3, 872−875

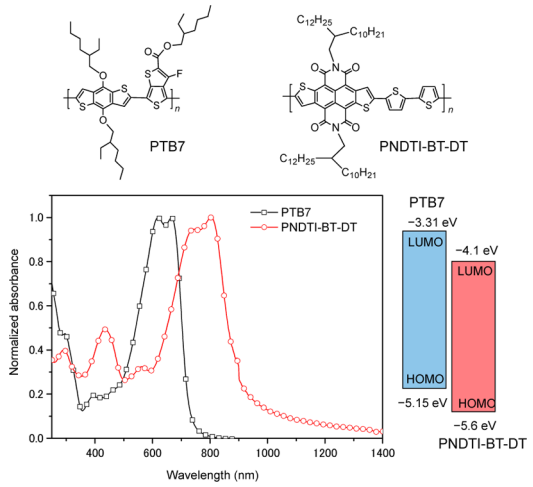

Figure 1. Chemical structures of PTB7 and PNDTI-BT-DT, together with their absorption spectra in film and energy level diagrams.

molecular orbital (LUMO) energy level of below −4 eV, which is sufficiently low as the acceptor materials for most of donor polymers. In addition, PNDTI-BT-DT exhibits high electron mobilities of up to 0.30 cm^2 V^{-1} s^{-1} in organic field-effect transistors. These properties indicate a great potential of PNDTI-BT-DT as the acceptor in all-PSCs. Herein, we report on the all-PSC based on PNDTI-BT-DT combined with poly[[4,8-bis[(2-ethylhexyl)oxy]benzo[1,2-*b*:4,5-*b*′]-bithiophene-2,6-diyl][3-fluoro-2-[(2-ethylhexyl)carbonyl]-thieno[3,4-*b*]thiophenediyl]] (PTB7), a donor polymer that has been extensively used in polymer/fullerene PSCs[13] and all-PSCs.[9e] We show that the all-PSCs demonstrate the high photoresponse in the NIR region comparable to the visible region.

The absorption spectra and the energy levels of the two polymers are shown in Figure 1. The pristine films of PTB7 and PNDTI-BT-DT have strong absorption bands in the regions of 500−750 nm and 600−900 nm, respectively. This complementary absorption spectra give a chance to utilize more sunlight, which is advantageous compared with the polymer/fullerene system. The highest occupied molecular orbital (HOMO) and LUMO energy levels of PNDTI-BT-DT are determined by cyclic voltammetry (CV) using the thin film and compared to those of PTB7.[13] The HOMO energy level of PNDTI-BT-DT by CV (−5.6 eV) is consistent with the data previously determined by photoelectron spectroscopy in air (−5.6 eV). The LUMO energy level estimated by CV (−4.1 eV) is higher-lying than that estimated by using the optically determined HOMO energy level and the optical band gap (−4.4 eV), reflecting the exciton binding energy. Here we use the energies obtained by CV for the discussion. The relatively large offsets of HOMO (0.45 eV) and LUMO (0.79 eV) between the polymers could lead to not only the effective photoinduced electron transfer from PTB7 to PNDTI-BT-DT but also the hole transfer from PNDTI-BT-DT to PTB7. Therefore, the photoresponse from both the polymers could be expected.

The photovoltaic performance of PTB7:PNDTI-BT-DT was investigated with a conventional sandwiched structure of glass/ITO/PEDOT:PSS/active layer/Ca/Al, where ITO and Ca/Al were the anode and the cathode, respectively. The active layers were spin-coated by using different solvents (CB, DCB, and CF) and the mixing ratios of PTB7 (donor; D):PNDTI-BT-DT

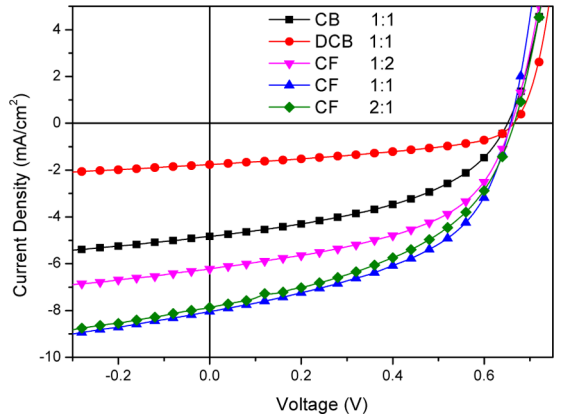

Figure 2. *J*−*V* curves under the AM 1.5 illumination (100 mW cm^{-2}) for PSCs based on the blend films of PTB7:PNDTI-BT-DT spin-coated from the different solvents.

Table 1. Device Characteristics of All-PSCs Fabricated with PTB7:PNDTI-BT-DT as the Active Layer

PTB7:PNDTI-BT-DT					
solvent	wt ratios	*V*OC (V)	J_{SC} (mA cm^{-2})	FF	PCE (%)
CB	1:1	0.66	4.84	0.45	1.42
DCB	1:1	0.66	1.76	0.44	0.51
CF	2:1	0.66	7.87	0.46	2.39
	1:1	0.66	8.05	0.49	2.59
	1:2	0.66	6.23	0.50	2.04
CF/DIO 99:1(v/v)	1:1	0.66	5.66	0.49	1.81

(acceptor; A) were accordingly optimized. The film thicknesses were in the range of 95−107 nm for all the films. The current density (*J*)-voltage (*V*) curves of the cells under the light irradiation are shown in Figure 2. Open-circuit voltage (V_{OC}), short-circuit current (J_{SC}), fill factor (FF), and PCE obtained from the *J*−*V* curves are summarized in Table 1. When CB and DCB were used as the solvent, all-PSCs showed relatively poor performances with low J_{SC} of 4.84 (PCE = 1.42%) and 1.76 mA cm^{-2} (PCE = 0.51%), respectively. Use of CF as the solvent gave the best J_{SC} of 8.05 mA cm^{-2}, and thus the PCE of 2.59% when the D−A ratio was 1:1 (w/w). The photovoltaic performance weakly depended on to the D−A ratios and PCE slightly decreased to 2.39 and 2.04% when the D−A mixed ratios were 2:1 and 1:2, respectively.

Figure 3 shows the external quantum efficiency (EQE) plots of the all-PSC under monochromatic light illumination. The shapes of the EQE curves of the devices with the D−A ratio of 1:1 (w/w) spin-coated by using the three solvents are similar to each other. The CF-used cell exhibits the highest EQE that is consistent with J_{SC}, in which the values reached 29% at ∼650 nm and 25% at 800 nm. Since the absorption onset of PTB7 is 750 nm, the photoresponse in the range of 750−950 nm undoubtedly comes from PNDTI-BT-DT with the EQE values comparable to the PTB7 region. This indicates that the use of PNDTI-BT-DT as the acceptor indeed enhanced NIR response compared with the other rylene imide-based acceptor polymers. This is probably due to the electron transfer from PTB7 at ground state to photoexcited PNDTI-BT-DT driven by HOMO−HOMO energy offset, as suggested by the energy diagram in Figure 1. The J_{SC} calculated from the integral of EQE curves is consistent with the experimental J_{SC} values under the simulated solar light (match within 3%).

dx.doi.org/10.1021/mz5004272 | *ACS Macro Lett.* 2014, 3, 872−875

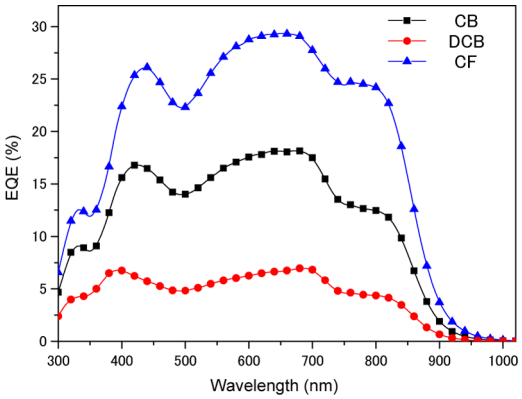

Figure 3. External quantum efficiency (EQE) plots of all-PSC based on PTB7:PNDTI-BT-DT spin-coated by using different solvents.

To investigate the difference in the photovoltaic performance of the cells using the three solvents, we observed the morphology of the three blend films by atomic force microscopy (AFM). Height images are shown in Figure 4.

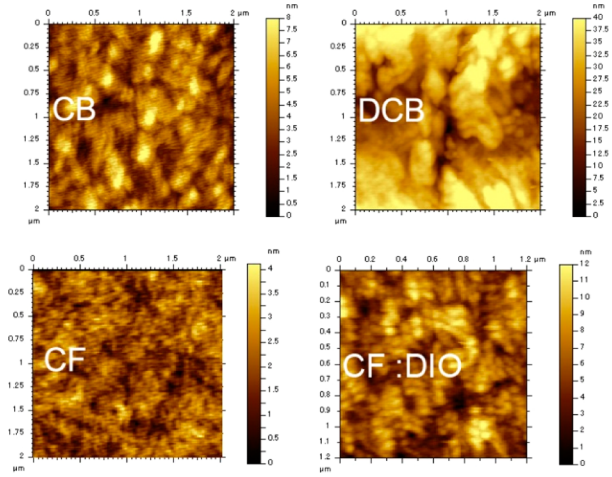

Figure 4. AFM height images of PTB7:PNDTI-BT-DT (1:1, w/w) composite films spin-coated by using the different solvents.

The blend films coated from CB and DCB solutions had obvious domain structures with root mean squares (rms) of 1.09 and 6.84 nm, respectively, suggesting severe phase separation between the polymers, especially in the case of DCB. In contrast, when CF was used as the solvent, the film had a rather smooth surface with rms of 0.48 nm, suggesting a more uniform mixing. For the reference, pristine PNDTI-BT-DT and PTB7 films coated from CB solutions showed smooth surfaces with rms of 0.458 and 0.435 nm, respectively. This difference in film morphology may be related to the miscibility of two polymers in these three solvents. The better morphology in the blend using CF should contribute to the charge separation efficiency and thus the highest PCE. Note that addition of small amount of 1,8-diiodooctane (DIO) to the solvent (1 vol %), which was previously reported to be effective to improve the PCE of all-PSCs,[9d,14] resulted in slightly larger grain size in AFM image with rms of 1.66 nm but the decrease of PCE to 1.81%.

Two-dimensional grazing incidence X-ray diffraction (2D GIXD) was measured to understand the crystallinity and orientation of both polymers in the pristine and blend film as

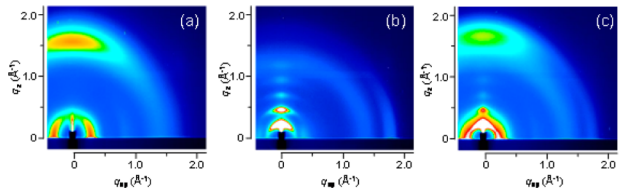

Figure 5. 2D GIXD patterns of the thin films: (a) pristine PTB7, (b) pristine PNDTI-BT-DT, and (c) PTB7:PNDTI-BT-DT (1:1, w/w) blend films.

shown in Figure 5. As previously reported, PTB7 was oriented in a face-on manner in the pristine polymer film, as the diffractions corresponding to the lamellar structure and the π-stacking appeared along the q_{xy} axis (q = 0.31 Å^{-1}, d = 20.3 Å) and the q_z axis (q = 1.60 Å^{-1}, d = 3.93 Å), respectively (Figure 5a).[15] In contrast, PNDTI-BT-DT film shows an edge-on orientation with the lamellar diffractions along the q_z axis (q = 0.23 Å^{-1}, d = 27.4 Å) and the π-stacking along the q_{xy} axis (q = 1.77 Å^{-1}, d = 3.54 Å; Figure 5b).[12] In the blend film, all the diffractions of PTB7 and PNDTI-BT-DT were independently appeared, indicating that the crystallinity and the orientation shown in the pristine films were maintained (Figure 5c). This suggests that, whereas PTB7 with preferential face-on orientation favorable for PSC application facilitates the hole transport, PNDTI-BT-DT with unfavorable edge-on orientation could be a disadvantage for the electron transport.[16] Nevertheless, the crystalline nature of PNDTI-BT-DT even in the blend film should greatly contribute to the charge separation at the interface between PTB7 and thus the high photoresponse in NIR region.

In conclusion, we demonstrated that, by using NDTI-based polymer, PNDTI-BT-DT, as the acceptor in combination with PTB7 as the donor, the all-PSC exhibited a high NIR response compared with that used other acceptor polymers reported so far. This can be attributed to the crystalline nature of PNDTI-BT-DT, though the orientation is unfavorable. Further molecular design to control the backbone orientation could lead to the higher performance of all-PSC. These results indicated that NDTI is a promising building unit for the design of new electron acceptor polymers for all-PSC application with higher efficiency.

EXPERIMENTAL SECTION

PTB7 with molecular weight (M_w) of 93000 and polydispersity (PDI) of 2.5 was purchased from 1-Material Inc. (Canada). PNDTI-BT-DT with M_w of 90400 and PDI of 3.3 was synthesized in our group. All-PSCs were fabricated with the conventional sandwich structure of glass/ITO/PEDOT:PSS/active layer/Ca/Al by several steps. PEDOT:PSS (Baytron P) was spin-coated (4000 rpm, 30 s) on the precleaned ITO substrate. The film was dried at 150 °C under a N_2 atmosphere for 5 min. After cooling the substrate, a blend solution of PTB7 and PNDTI-BT-DT with the total concentration of 15 g L^{-1} was spin-coated. The substrate was annealed at 80 °C for 30 min inside a nitrogen-filled glovebox to dry the solvent completely, after which a Ca/Al (20 nm/60 nm) electrode was evaporated onto the substrate under high vacuum (<2 × 10^{-4} Pa) in an evaporation chamber (ALS Technology, H-2807 vacuum evaporation system with E-100 load lock). Photovoltaic cells without protective encapsulation were subsequently tested in air under simulated AM1.5 solar irradiation (100 mW cm^{-2}, Peccell Technologies, PCE-L11). The light intensity was adjusted by using a standard silicon solar cell with an optical filter (Bunkou Keiki, BS520). The current–voltage characteristics of the photovoltaic cells were measured using a Keithley 2400 I–V measurement system. The external quantum efficiency (EQE) of the

dx.doi.org/10.1021/mz5004272 | ACS Macro Lett. 2014, 3, 872–875

devices was measured on a Hypermonolight System (Bunkou Keiki, SM-250F).

The configuration of the shadow mask afforded eight independent devices on each substrate, with an active layer of ~0.21 cm^2 (3 mm × ~7 mm) for each device. The effective area of the PSCs was accurately defined using a metal photomask (2 mm × 3 mm) during irradiation with simulated solar light. 2D GIXD measurements were conducted at the SPring-8 on beamline BL19B2 with an X-ray energy of 12.39 keV (λ = 1 Å). The sample was irradiated at a fixed incident angle of 0.12° through a diffractometer (Huber), and the GIXD pattern was recorded with a Pilatus 300 K 2D image detector (Dectris). CV of PNDTI-BT-DT film was measured ALS Electrochemical Analyzer Model 612D in benzonitrile containing tetrabutylammonium hexafluorophosphate (Bu_4NPF_6, 0.1 M) as supporting electrolyte at a scan rate of 100 mV/s. Counter and working electrodes were made of Pt, and the reference electrode was Ag/AgCl. AFM images were taken on a 5500 scanning probe microscope (Agilent Technologies) in AC mode.

AUTHOR INFORMATION

Corresponding Authors

*E-mail: takimiya@riken.jp.

*E-mail: keisuke.tajima@riken.jp.

Notes

The authors declare no competing financial interest.

ACKNOWLEDGMENTS

This work was supported in part by the New Energy and Industrial Technology Development Organization (NEDO), Japan. 2D-GIXD experiments were performed with the approval of the Japan Synchrotron Radiation Research Institute (JASRI; Proposal 2013A1634). The authors thank Dr. T. Koganezawa (JASRI) for supporting the 2D GIXD measurements.

REFERENCES

(1) (a) Li, Y.; Zou, Y. *Adv. Mater.* **2008**, *20* (15), 2952−2958. (b) Dennler, G.; Scharber, M. C.; Brabec, C. J. *Adv. Mater.* **2009**, *21* (13), 1323−1338. (c) Zhou, H.; Yang, L.; You, W. *Macromolecules* **2012**, *45* (2), 607−632.

(2) (a) Sun, Y.; Welch, G. C.; Leong, W. L.; Takacs, C. J.; Bazan, G. C.; Heeger, A. J. *Nat. Mater.* **2012**, *11* (1), 44−48. (b) Zhou, J.; Zuo, Y.; Wan, X.; Long, G.; Zhang, Q.; Ni, W.; Liu, Y.; Li, Z.; He, G.; Li, C.; Kan, B.; Li, M.; Chen, Y. *J. Am. Chem. Soc.* **2013**, *135* (23), 8484−8487. (c) He, Z.; Zhong, C.; Su, S.; Xu, M.; Wu, H.; Cao, Y. *Nat. Photonics* **2012**, *6* (9), 593−597.

(3) (a) McNeill, C. R.; Greenham, N. C. *Adv. Mater.* **2009**, *21* (38−39), 3840−3850. (b) Facchetti, A. *Mater. Today* **2013**, *16* (4), 123−132. (c) Anthony, J. E. *Chem. Mater.* **2011**, *23* (3), 583−590.

(4) Halls, J.; Walsh, C.; Greenham, N.; Marseglia, E.; Friend, R.; Moratti, S.; Holmes, A. *Nature* **1995**, *376* (6540), 498−500.

(5) (a) Granström, M.; Petritsch, K.; Arias, A.; Lux, A.; Andersson, M.; Friend, R. *Nature* **1998**, *395* (6699), 257−260. (b) Holcombe, T. W.; Woo, C. H.; Kavulak, D. F.; Thompson, B. C.; Frechet, J. M. *J. Am. Chem. Soc.* **2009**, *131* (40), 14160−14161.

(6) Mori, D.; Benten, H.; Ohkita, H.; Ito, S.; Miyake, K. *ACS Appl. Mater. Interfaces* **2012**, *4* (7), 3325−3329.

(7) Li, W.; Roelofs, W. S.; Turbiez, M.; Wienk, M. M.; Janssen, R. A. *Adv. Mater.* **2014**, *26* (20), 3304−3309.

(8) (a) Zhan, X. W.; Tan, Z. A.; Domercq, B.; An, Z. S.; Zhang, X.; Barlow, S.; Li, Y. F.; Zhu, D. B.; Kippelen, B.; Marder, S. R. *J. Am. Chem. Soc.* **2007**, *129* (23), 7246−7247. (b) Zhou, E.; Tajima, K.; Yang, C.; Hashimoto, K. *J. Mater. Chem.* **2010**, *20* (12), 2362−2368. (c) Zhou, E.; Cong, J.; Wei, Q.; Tajima, K.; Yang, C.; Hashimoto, K. *Angew. Chem., Int. Ed.* **2011**, *50* (12), 2799−2803. (d) Zhou, Y.; Kurosawa, T.; Ma, W.; Guo, Y.; Fang, L.; Vandewal, K.; Diao, Y.; Wang, C.; Yan, Q.; Reinspach, J. *Adv. Mater.* **2014**, *26* (22), 3767−3772.

(9) (a) Fabiano, S.; Chen, Z.; Vahedi, S.; Facchetti, A.; Pignataro, B.; Loi, M. A. *J. Mater. Chem.* **2011**, *21* (16), 5891−5896. (b) Zhou, E.; Cong, J.; Zhao, M.; Zhang, L.; Hashimoto, K.; Tajima, K. *Chem. Commun.* **2012**, *48* (43), 5283−5285. (c) Earmme, T.; Hwang, Y.-J.; Murari, N. M.; Subramaniyan, S.; Jenekhe, S. A. *J. Am. Chem. Soc.* **2013**, *135* (40), 14960−14963. (d) Zhou, E. J.; Cong, J. Z.; Hashimoto, K.; Tajima, K. *Adv. Mater.* **2013**, *25* (48), 6991−6996. (e) Mori, D.; Benten, H.; Okada, I.; Ohkita, H.; Ito, S. *Adv. Energy Mater.* **2014**, *4* (3), 1301006. (f) Earmme, T.; Hwang, Y.-J.; Subramaniyan, S.; Jenekhe, S. A. *Adv. Mater.* **2014**, DOI: 10.1002/adma.201401490. (g) Mori, D.; Benten, H.; Okada, I.; Ohkita, H.; Ito, S. *Energy Environ. Sci.* **2014**, DOI: 10.1039/C4EE01326C.

(10) Schubert, M.; Dolfen, D.; Frisch, J.; Roland, S.; Steyrleuthner, R.; Stiller, B.; Chen, Z.; Scherf, U.; Koch, N.; Facchetti, A.; Neher, D. *Adv. Energy Mater.* **2012**, *2* (3), 369−380.

(11) Zhou, E.; Hashimoto, K.; Tajima, K. *Polymer* **2013**, *54* (24), 6501−6509.

(12) Fukutomi, Y.; Nakano, M.; Hu, J.-Y.; Osaka, I.; Takimiya, K. *J. Am. Chem. Soc.* **2013**, *135* (31), 11445−11448.

(13) Liang, Y.; Xu, Z.; Xia, J.; Tsai, S. T.; Wu, Y.; Li, G.; Ray, C.; Yu, L. *Adv. Mater.* **2010**, *22* (20), E135−8.

(14) Hwang, Y.-J.; Ren, G.; Murari, N. M.; Jenekhe, S. A. *Macromolecules* **2012**, *45* (22), 9056−9062.

(15) Szarko, J. M.; Guo, J.; Liang, Y.; Lee, B.; Rolczynski, B. S.; Strzalka, J.; Xu, T.; Loser, S.; Marks, T. J.; Yu, L.; Chen, L. X. *Adv. Mater.* **2010**, *22* (48), 5468−5472.

(16) (a) Guo, J.; Liang, Y.; Szarko, J.; Lee, B.; Son, H. J.; Rolczynski, B. S.; Yu, L.; Chen, L. X. *J. Phys. Chem. B* **2010**, *114* (2), 742−748. (b) Osaka, I.; Kakara, T.; Takemura, N.; Koganezawa, T.; Takimiya, K. *J. Am. Chem. Soc.* **2013**, *135* (24), 8834−8837.